Electronic Supplementary Information for "Optimal Control with Homologous Families of Photonic Reagents and Chemical Substrates"

Katharine Moore Tibbetts, Xi Xing, and Herschel Rabitz

April 21, 2013

This supplemental material presents some additional experimental data regarding the intensity-dependence of the objective yields not included in the main work. The main work presented plots of objective yields versus laser intensity for the Class I-III objectives in CH_2BrCl over large samples of trial photonic reagents (Figure 2). The latter plots showed that a wide range of objective values was observed at sufficiently low laser intensity. Here, we show that TOF spectra at the same fractional integrated laser intensity $I^2/I_0^2 = 0.078 \pm 0.003$ (where I_0^2 denotes the TPA signal of the 360μJ TL pulse) exhibit significant differences from three distinct shaped pulses, as presented in Figure S.1. Spectrum (a) comes from the 90μJ TL pulse, with a high yield of CH_2Cl^+ and small yields of other products. The spectrum (b) was obtained from an optimal pulse (energy 360μJ) in the pixel basis for the Class II objective and exhibits a similar CH_2Br^+ ion yield as in (a), but approximately one third of the CH_2Cl^+ yield along with significantly higher yields of Cl^+ and Br^+. Spectrum (c) was obtained from an optimal pulse (energy 360μJ) in the polynomial basis for the Class I objective, which exhibits significantly reduced yields of CH_2Cl^+ and CH_2Br^+ as compared to Cl^+ and Br^+. The significant differences in the TOF mass spectra for different pulse shapes with the same intensity suggest that the intensity only plays a limited role in determining the fragmentation pattern.

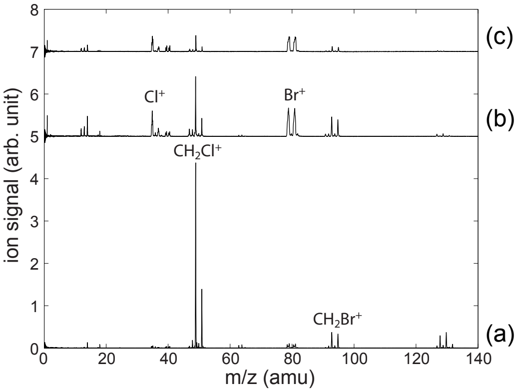

Figure S.1: TOF spectra of CH_2BrCl from photonic reagents with intensity $I^2/I_0^2 = 0.078 \pm 0.003$ on the normalized abscissa of Figure 2 of the main work: (a) TL pulse with pulse energy of 90μJ, (b) optimal pulse of 360μJ in the pixel basis for the Class II objective, and (c) optimal pulse of 360μJ in the polynomial basis for the Class I objective. Selected ionic species are labelled. The three spectra are shown to scale and have dramatically different total ion yields and relative yields of the labelled ion fragments.

We also present in Figure S.2 the analogous correlation with laser intensity for the Class I-III objectives in CH_2ICl, where the photonic reagents were sampled by scanning the TL pulse energy (black circles), from a pixel basis GA optimization (red squares), and from a polynomial basis GA optimization (blue triangles). The general features resemble the corresponding plot for CH_2BrCl (Figure 2 of the main work), with wide ranges of observed objective values at sufficiently low laser intensity. As was the case for CH_2BrCl, optimization with the polynomial basis achieves a higher yield of the Class I objective than with the pixel basis, but the yields obtained for the Class II and III objectives are similar. Analogous correlation plots for other substrates exhibit similar structure (not shown), illustrating a further homologous property variation across the halomethane family.

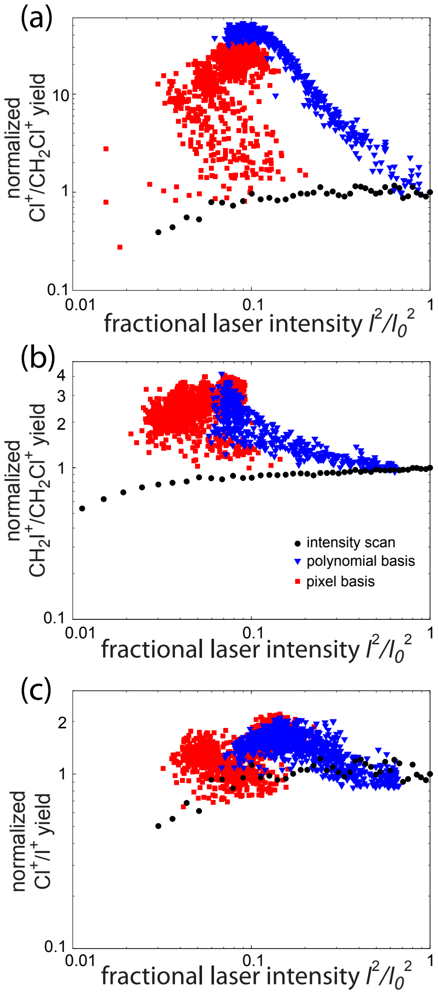

Figure S.2: Objective yields versus laser intensity for CH$_2$ICl: (a) Class I objective, (b) Class II objective, and (c) Class III objective. Both the objective on the ordinate and laser intensity on the abscissa are normalized to unity at the full-energy (360μJ) TL pulse. The black circles denote objective yields obtained from scanning the laser pulse energy with the TL phase. The red squares denote objective yields obtained over the course of a GA optimization with the pixel basis, and the blue triangles denote objective yields obtained over the course of a GA optimization with the polynomial basis. The maximal objective yields on these plots are higher than the yields reported in Table I of the main work because they were averaged only over 500 laser shots here, instead of 50,000 laser shots, as in Table I.

Finally, we present the statistical distributions of Class I objective yields under interaction with an optimal photonic reagent $\Phi(\omega)$ and the time-reversed optimal photonic reagent $-\Phi(\omega)$. The intensity (i.e., TPA signal) should not change upon time-reversal. In our time-reversal experiments, the respective TPA yields from $\Phi(\omega)$ and $-\Phi(\omega)$ deviated by less than 3%, which was within the noise of the TPA yield. Figure S.3(a) shows the statistical distributions of unnormalized Class I objective yields of Cl^+/CH_2Cl^+ in CH_2ICl from an optimal pulse ("opt," $I^2/I_0^2 = 0.078$, blue, dashed line), time-reversed optimal pulse ("rev," $I^2/I_0^2 = 0.076$, red, dotted line), and TL pulse (black, solid line). Dividing the optimal and time-reversed distributions by the mean of the black distribution gives the mean normalized objective yields $\mu_{opt} = 30.3$ (c.f., Table 1 of the main work) and $\mu_{rev} = 10.8$. The corresponding mass spectra from the optimal and time-reversed pulses are given in Figure S.3(b). The blue box shows that upon time-reversal, the Cl^+ signal is nearly the same for spectra from the optimal pulse (top) in time-reversed pulse (bottom). The red box shows that the CH_2Cl^+ signal more than doubles upon time-reversal. Thus, the time-ordering of the optimal spectral phase serves to decrease the yield CH_2Cl^+.

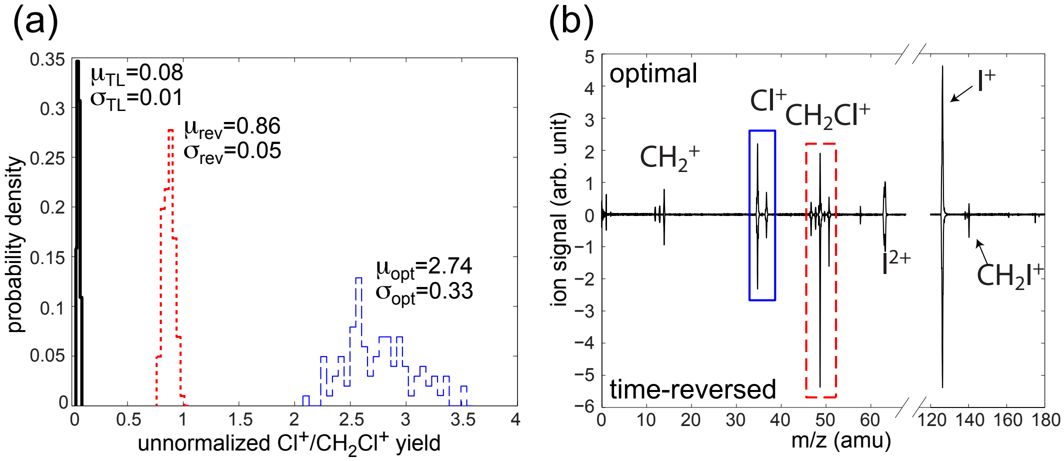

Figure S.3: Illustration of the importance of spectral time-ordering of the photonic reagent in the Class I objective. (a) Probability distributions of *unnormalized* (see text for explanation) objective yields obtained for CH_2ICl with an optimal photonic reagent (blue, dashed line), the time-reversed optimal photonic reagent (red, dotted line), and TL pulse (black, solid line). Mean and standard deviation values for each distribution averaged over 100 samples of 500 laser shots each are indicated. (b) Mass spectra from the optimal (top) and time-reversed (bottom) photonic reagents. The blue (solid) box shows that the Cl^+ yield is almost the same, while the red (dashed) box shows that the CH_2Cl^+ yield grows by more than a factor of two under interaction with the time-reversed photonic reagent.